Adsorption
https://doi.org/10.1007/s10450-024-00520-4

Environment benign *Ghee* residue – titania based adsorbent for quick removal of methyl orange dye

Meenal Joshi[1] · Abhijeet R. Kadam[2] · S. J. Dhoble[3]

Received: 10 May 2024 / Revised: 29 June 2024 / Accepted: 4 July 2024

Abstract
Use of renewable waste material for water treatment is an area of interest. An attempt has been made for preparation of Dairy industry waste *Ghee* residue (GR) based biogenic adsorbent for removal of dye present in water/waste water. This novel approach contributes in valorisation of dairy industry by- product *Ghee* residue. The *ghee* residue was first converted into carbon and processed with the titanium precursor and rare earth metal. This combination yields GR-C/TiO_2/Eu^{3+} adsorbent. A series of adsorbing material was prepared by differing loading of Eu^{3+} keeping ratio of RG-C and TiO_2 constant. Synthesized adsorbents were subjected to characterization studies such as X-Ray Diffraction (XRD) spectroscopy, Brunauer Emmett Teller-Surface Area (BET-SA), Scanning Electron Microscopy (SEM), Fourier Transformed Infra Red spectroscopy (FTIR) etc. XRD pattern shows formation of crystalline anatase phase of TiO_2 with average particle size of 34.9494 nm. SEM image also confirms irregular morphology with particles in nanometer range. BET-surface area of GR-C/TiO_2/Eu^{3+} (1%) was found to be 53.633 m^2/g with total pore volume = $8.555e^{-02}$ cc/g for pores smaller than 18330.1 Å (Radius) at P/Po = 0.99948 and average pore radius was found to be $3.19022e^{+01}$ Å indicating mesoporosity of material. Synthesized adsorbents were studied for dye adsorption and GR-C/TiO_2/Eu^{3+} (1%) shows quick and complete removal of 5ppm Methyl orange dye in contact time of less than three minutes at 30-32°C with the adsorbent dose of 75 mg/10mL. The high adsorption property is attributed to presence of crystalline nanostructured TiO_2 and Eu^{3+} on to the biogenic carbon framework. Langmuir adsorption isotherm data indicates monolayer adsorption with R^2 value of 0.97. ΔG^o values are in the range of -12.81 to -17.77 KJ mol^{-1} indicating spontaneous adsorption process.

Keywords Adsorption · TiO_2 · Ghee residue · Dye removal · Adsorbent

1 Introduction

Dyes have been used worldwide for different applications by various industries such as food, cosmetics, textiles, medical sector, tanneries etc. About 7.5 metric tons of dyes have been discharged by dyeing industries annually [1] in the environment. Apart from imparting colour, presence of dye has several other disadvantages on aquatic as well as human life [2]. Modern synthetic dyes are strong and long lasting; they are non biodegradable and found to be carcinogenic to humans [3]. They remain in the environment and enter into the food chain via bioaccumulation and their concentration increases by bio magnification in the upper level of food chain. There are various categories of dyes depending on the charges they bear such as cationic, anionic and non-ionic [4]. Azo dyes are worth mentioning here as about 50% dyes used as colourant are azo dyes. –N = N- bond present in azo dye is not easily soluble and is toxic in nature (IUPAC 997). Methyl orange dye is selected here owing to its utilization in textile, laboratories as indicator, printing of paper, pharmaceuticals and food industries. Methyl orange is anionic dye, mostly identified as sulphonated azo dye. In addition to this methyl orange is carcinogenic, mutagenic, teratogenic [5] and presence of sulpho and azo group imparts recalcitrant character to the compound [6]. Presence of azo dyes into the

✉ Meenal Joshi
meenal5125@gmail.com

[1] Department of Chemistry, Shri Ramdeobaba College of Engineering and Management, Nagpur 440013, India

[2] Department of Physics, CSMSS's Chh. Shahu College of Engineering, Chhatrapati Sambhajinagar, Aurangabad 431011, India

[3] Department of Physics, R.T.M. Nagpur University, Nagpur 440033, India

Published online: 28 July 2024

water and waste water shows various health impacts from mild symptoms such as eye irritation, nausea to dysfunctions of kidney, liver and nervous system [7]. Therefore, is important to look for treatment strategies for dye removal from waste water before its discharge into the ecosystem in the view of sustainable development.

Presence of no. of azo groups into the compound makes the dye more tolerant to the remediation techniques however various dye removal techniques are studied by researchers such as adsorption [8], ion exchange [9], oxidation [10], membrane filtration, biological, photocatalytic [11] etc. Most of the methods are complex and cost effective however adsorption is most widely studied because of simple design, high efficiency, no waste generation and being economic process [12, 13]. Activated charcoal, carbon is the most reported adsorbents with or without modifications and functionalization [14]. Various biodegradable adsorbents are now extensively studied and reported [15, 16] with advantage of degrading back in the environment.

Various bioinspired adsorbents were reported in literature, M. H. Rahman et-al [17] in 2021 reported synthesis of modified cellulose and chitosan based adsorbent and applied for removal of heavy metals such as Cr, Pb and Cd. However, removal rate is for Cr, Pb and Cd is 56, 85 and 94% respectively with metal concentration 60 ppm with adsorbent dose of 1.0 gmL^{-1} at pH 4. Composite shows maximum adsorption of 55, 80 and 91 mg/g at pH-4, with metal concentration 120 ppm and 1.0 gmL^{-1} for Cr, Pb and Cd respectively. Citrus peel unmodified and modified with calcium alginate were reported by Amina Aichour et-al [18] for removal of methylene blue and the adsorption capacity is found to be 185.83 and 964.54 mg/g respectively for without and with modification. The highest bed capacity reported here is of 31.45 mg/g with 93.6% dye treated using 2 ml/min rate flow, 200 mg/L inlet methylene blue concentration and 3.5 cm (4 g) bed height. R. Malik (2007) identified ground nut shell waste for synthesis of activated carbon and applied for removal of malachite green via adsorption technique [19]. Groundnut shell powered activated carbon showed 94.5% dye removal in 30 min at a dose of 0.5 g/L with initial dye concentration of 100 mg/L. Eco friendly adsorbent was also reported from mint waste [20] and applied for removal of hexavalent Chromium with removal percentage of 41–98% and highest removal was observed at pH = 2 with initial dye concentration of 10 mg/L. Unriped plant fruits [21], plant bark lactine [22], egg shell waste [23], soya waste [24], almond shell [25], etc. are also reported for effective removal of dyes and heavy metals. Reports are also obtained for Asphaltenes from Asphalt Rocks for synthesis of adsorbent by Zhenwei Han in 2019 [26] However combination of biogenic carbon with titania has not been reported.

TiO_2 is known as very promising material for adsorption due to low cost, high surface area and environmental benign nature. As adsorption is surface phenomenon mostly based on surface characteristics, TiO_2 shows interfacial electron transfer process during chemisorptions. In the presence of water, co-ordination vacancies on the surface of TiO_2 crystal are occupied by water forming amphoteric titanol group (=Ti-OH) [27]. Dyes/contaminants present in the water can be easily adsorbed on the surface via surface hydroxyl groups [28]. Chuanyong Jing et al. [29] synthesized nanocrystalline titania via classical method and applied for adsorption of As(V), As (III), monomethylarsonic acid (MMA), and dimethylarsinic acid (DMA) present in ground water. Initial concentration of ions are 329 mg/L for As(III), 246 mg/L for As(V), 151 mg/L for MMA, and 202 mg/ L for DMA, contact time 6 min for 4 months. Around 11 000, 14 000, and 9900 bed volumes of water had been treated before As (V) & (III), MMA concentration in treated water to reach 10 µg/L, however very small recovery was observed in case of DMA. Amorphous sodium titanite was reported by Katerina Fialova [30] for removal of Manganese present in drinking water. Demanganization was observed at pH = 7 with q_e = 73.83 mg/g, the process involves adsorption as well as ion exchange. Metal oxide/TiO_2 was also reported in literature for adsorption of H_2S gas at high temperature (480°C) using wet impregnation method NiO/TiO_2, CuO/TiO_2, and CoO/TiO_2 nanocompositeds were prepared by author [31], best results were observed for metal to TiO_2 ratio of 2.5/5 with initial concentration of H_2S 2000ppm, and fed flow rate of 17 cc/min.

A. A. Aziz et al. [32] synthesized nitrogen doped titania and activated carbon as synergistic compound containing improved composite for adsorption-photocatalytic oxidation of Batik dye Remazol Brilliant Blue (RBB). Activated carbon used here is the commercially available one with high surface area. Compound shows removal efficiency of 80% in 6 h under direct solar radiation with catalyst dose of 1 g and 50 mg/L initial dye concentration. Zhao et al. (2020) [33] reported carbon doped titanium oxide from polytitanium coagulated sludge for photocatalytic as well as adsorption of pollutants. Two types of carbon doped titania were obtained, C-TiO_2 (with low C content) and C-TiO_2 (with high C content). The pollutants selected were Rhodamine blue and methyl orange. C-TiO_2 (with high C content) functioned as adsorbent showed removal efficiency for RB and MO about 98% in 20 min and C-TiO_2 (with low C content) functioned as photocatalyst degraded RB and MO 99.6 and 97.0% respectively from initial concentration 20 mg/L in 210 min.

In present study we have synthesized *ghee* residue-Titania based adsorbent with Eu doping. *Ghee* residue is a dairy waste formed during *ghee* (clarified butter Fat) preparation,

with limited food applications due to dark colour in spite of antioxidant properties [34]. This is rich in mineral content apart from energy and protein. Chemical composition contains dry protein 25%, calcium 0.88% and phosphorous 0.50% [35]. Dairy industry is mostly encouraging non food applications for valorisation due to presence of dark brown colour of *ghee* residue. Using surface modified *ghee* residue protien Linlin Hao [36] reported removal of hazardous metals As (V), Cu(II) and P(V) from water. Author removed fat content of waste and surface is functionalized with polyethylenimine (PEI) and Fe(III) ions. Maximum absorption capacity reported were 45.1, 80.7 and 21.7 mg/g for As (V), Cu(II) and P(V) respectively with 100 mg/L initial ion concentration and pH = 5. In the present study we propose, use of as such *ghee* residue as a biogenic support for porous titania based adsorbent preparation. Crystalline titania with porous support of *ghee* residue carbon along with Eu doping was synthesized under inert environment at 400°C. *Ghee* residue to TiO_2 ratios was varied from 1:1 to 1:2 and doping of Eu was also varied as 0.25 to 1 and 1.5%. This black coloured composite is showing unexpectedly high adsorption property when studied for removal of methyl orange dye. The adsorption is so quick that complete removal is observed within 2 min 24 s with initial dye concentration of 5ppm at pH = 7 and 30°C temperature.

2 Synthesis

2.1 Synthesis of GR based adsorbent

2 g of *ghee* residue preheated at 300°C was taken in a 100mL beaker. 11.8425 g of Titanium isopropoxide was weighed and mixed with preheated *ghee* residue. Mixture was stirred for 30 min on stirrer for homogeneous dispersion of Titanium -isopropoxide, resultant solution is labelled as C-Ti solution. 0.068 g of Eu_2O_3 was dissolved in minimum quantity of conc. HNO_3 and heated in oven at 60°C in order to achieve clear solution. This Eu-nitrate solution was then mixed with C-Ti solution and stirred for 20 min. This reaction mixture is kept in oven at 150 °C for 30 min; thick mass was obtained which was further reduced in furnace at 800 °C.

Series of Eu doped material were synthesized by various the concentration of Eu from 0.5 to 1.5% with an increment of 0.25%.

2.2 Adsorption of methyl orange dye

The as synthesized materials were subjected for adsorption of methyl orange dye. A 10 ml, 5 ppm methyl orange solution was taken in a conical flask of 50 mL capacity and a known weight of as synthesized material was added into it. Flask was kept on stirrer for continuous stirring. A stop watch was simultaneously kept on so that the time required for decolourization can be monitored. After a complete decolourization of solution, it was filtered and analysed on spectrophotometer at 464 nm wavelength. Adsorption is measured in terms of % MO adsorption as follows:

$$\%M.O.adsorption = \frac{C_{Initial} - C_{Final}}{C_{Initial}} \times 100$$

Above mentioned procedure is followed for screening and short listing of adsorbent and studying effect of various operational parameters on adsorption process.

2.3 Characterization

Synthesized adsorbents were subjected to different characterization techniques, XRD was carried out on Regaku minflex d 600 x-ray diffractometer with Cu Kα radiation with λ = 0.154056 nm operated at 40 kV, 15mV. Brunauer Emmett Teller-Surface Area (BET-SA), total pore size and average pore volume was analysed out on Quantachrome Nova station B Surface area analyser at 77 K. Surface area was calculated by BET method and pore size and pore volume is calculated by Barrett-Joyner-Halenda (BJH) method. Surface morphology and particle shape was analysed on Scanning Electron Microscope instrument, Model no. Carl Zeiss EVO-18. FTIR spectra of as synthesized adsorbent were recorded on Bruker Vertex- 70 using diffused reflectance accessory technique. Dye sample Concentration before and after adsorption was carried out on UV- Vis- NIR Spectrophotometer, Make-Aimil at 464 nm.

3 Result and discussion

3.1 XRD analysis

X-ray diffraction pattern of C-GR/TiO_2 (1:1)/ Eu(0.25%), C-GR/TiO_2 (1:1)/Eu(0.5%), C-GR/TiO_2 (1:1)/Eu(0.75%), C-GR/TiO_2 (1:1)/Eu(1%) and C-GR/TiO_2 (1:1)/Eu(1.5%) was shown in Fig. 1. The XRD profiles of prepared adsorbents are in good agreement with the standard ICSD database card number 00-001-0562 [37]. Moreover, there are some additional peaks were observed positioned at 38 °, 34 ° and 45 ° may be due to residual carbon present in the material.

As the XRD peaks shows crystalline nature of the sample. Crystallite sizes were calculated using Dybye–Scherrer equation given in Eq. 1;

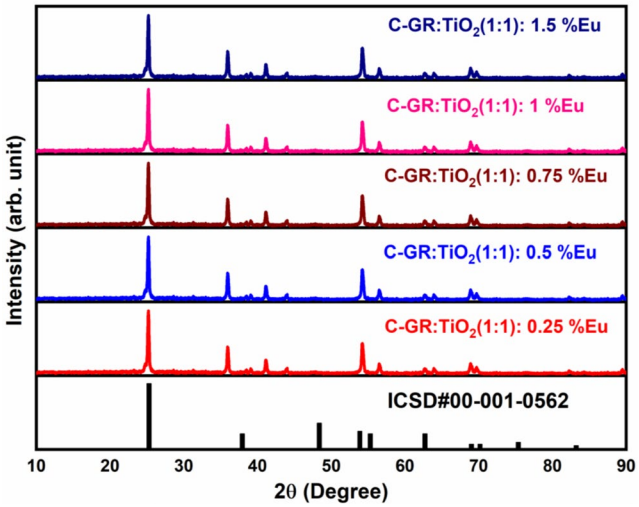

Fig. 1 X-ray diffraction pattern of C-Gr /TiO_2 (1:1): Eu(0.25%), C-GR/TiO_2 (1:1): Eu(0.5%) and C-GR/TiO_2 (1:1): Eu(0.75%), C-GR/TiO_2 (1:1):Eu(1%) and C-GR/TiO_2 (1:1):Eu(1.5%)

$$D = \frac{k\lambda}{\beta \cos \theta} \quad (1)$$

Where D is the crystallite size (nm), k is a constant (0.94 for spherical particles), λ is the wavelength of the X-ray radiation (CuKα = 0.1541 nm), β is the full width at half maximum (FWHM) of the intense and broad peaks, ε is the lattice strain while θ is the Bragg's or diffraction angle. The average particle size of proposed sample is found to be 34.9494 nm. Hence, we conclude that the prepared sample is in nanometric size.

Anantase phase of titania is polymorphic form of titania where each titanium cation is in coordination with six oxygen anions in slightly distorted octahedron shape and each oxygen is co-ordinated to three titanium cation in equilateral triangle shape. Surface area of anatase form is greater than any other form of titania such as rutile therefore anatase phase can show more activity towards adsorption [38]. Michele E. Barbour in 2007 reported that anatase phase is effective than rutile phase for adsorption of Chlorhexidine [39].

Sharp peaks with high peak intensities were observed for all the XRD patterns indicate formation of high crystallinity with nano particle size. Phase and particle size are mostly enhancing physical properties of material [40].

3.2 BET-SA

Surface area, pore size and pore volume were calculated on Quantachrome Nova Station B instrument at 77 K. Surface area was calculated by using Brunauer–Emmett–Teller (BET) nitrogen adsorption-desorption method and pore size using Barrett–Joyner–Halenda (BJH/DH) method adsorbate model. Adsorption isotherm, Multipoint BET Plot and BJH desorption curve for synthesized adsorbent are shown in Figure:2. BET isotherm follows type IV with hystyresis for desorption corresponds to mesoporosity of material [41] and BET-SA plot shows excellent linearity with intercept value of -1.577e-02 1/g. Multipoint surface area of C-GR / TiO_2 (1:1)/ Eu (1%) was found to be 53.633 m^2/g.

BJH desorption size distribution curve shows total pore volume of about 8.555e-02 cc/g for pores smaller than 18330.1 Å (Radius) at P/Po = 0.99948 and average pore radius of about 3.19022e + 01 Å. As per the pore size classification for BET theory pore size between 1 and 10 nm falls under mesoporous category so the pores of synthesized adsorbent are found to be mesoporous in nature.

The surface area values are quite less in comparison to the commercially available activated carbon i.e., 600-1200 m^2/g [42]. However presence of porous morphology, high crystalinity and addition of cationic species such as titania and Eu on to the carbon framework attributed to the high adsorption capacity of the material.

3.3 SEM

Surface analysis and morphology of GR/TiO_2 (1:1)/ Eu (1%) was carried out by using Scanning electron microscopy and details are shown in Fig. 3. SEM images shows irregular morphology of a C-GR/TiO_2 (1:1) /Eu (1%) also particles with irregular shape and sizes were observed however few particles were found at nanometer level from 82.45 nm to 145.4 nm ranges. No regular pattern for synthesized adsorbent was observed however mostly round to oval shaped particles were observed. Agglomeration of smaller particles to form a large bulk particle can also be seen in SEM images.

3.4 FTIR

Fourier transform Infrared spectra of C-GR/TiO_2 (1:1)/ Eu (1%) before and after adsorption process was recorded from 400 to 4000 cm^{-1} and presented in Fig. 4. In case of C-GR/TiO_2 (1:1)/ Eu (1%) before adsorption (Fig. 4 (a)) 15 major peaks were observed at 442.68, 553.59, 676.08, 1118.76, 1383.98, 1534.44, 1601.95, 1948.19, 2357.11, 3436.33, 3512.52, 3601.25, 3727.6, 3857.8 and 3965.82 cm^{-1}. Peak at 442.68 indicates Eu-O stretching vibrations [43] Peak around 550 cm^{-1} (553.59 cm^{-1}) corresponds to Ti-O vibration transitions [44], Peak around 650 cm^{-1} (676) corresponds to the presence of TiO_2 in the matrix [45]. Peak at 1118.76 cm^{-1} corresponds to Ti-O-C stretching vibrations [46]. This peak confirms inclusion of Titania into the ghee residue matrix. Peaks at 1383.98, 1534.44, 1601.95, 3436.33, 3512.52, 3601.25, and 3727.6, cm^{-1} corresponds

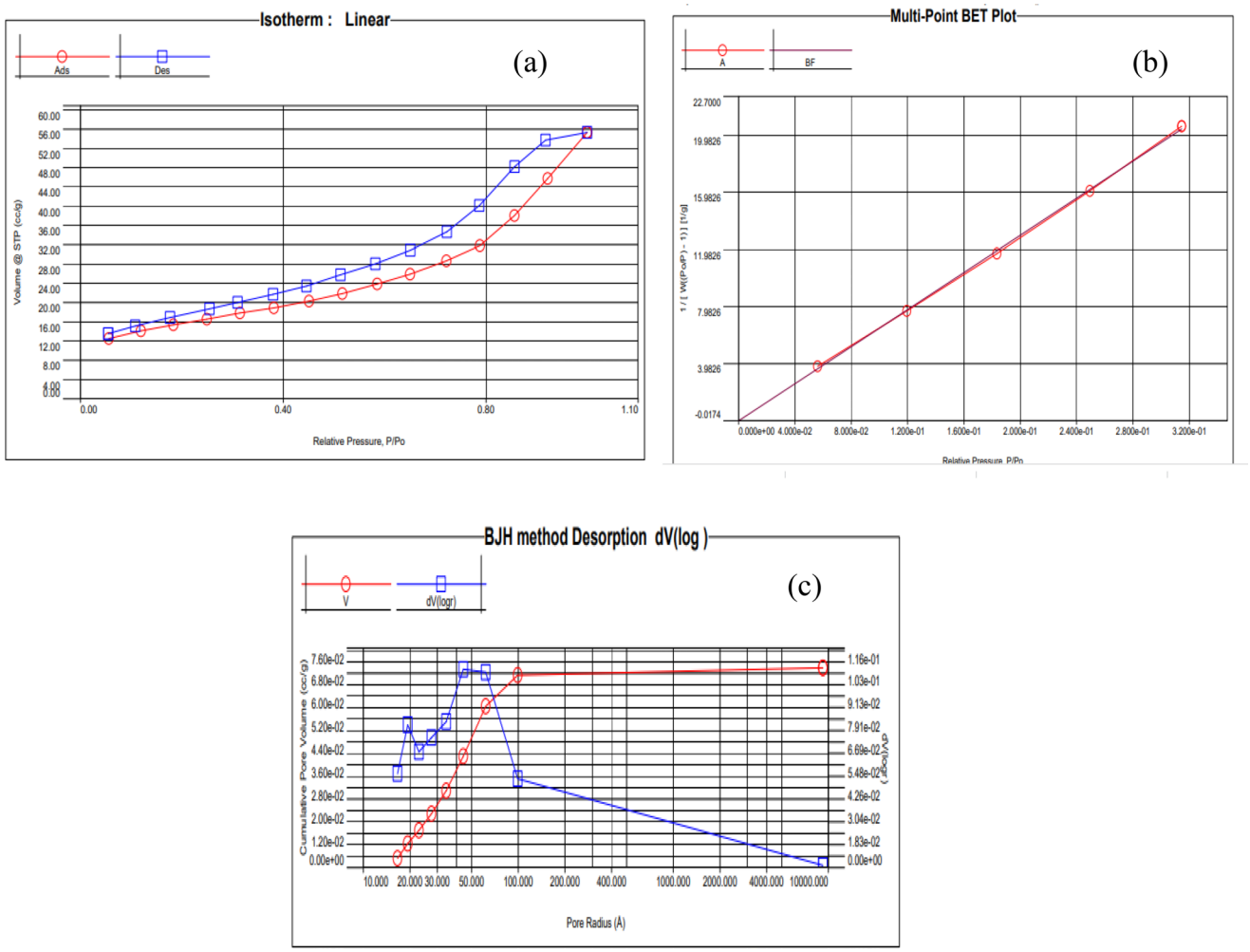

Fig. 2 Plots for (**a**) BET Isotherm, (**b**) multi-point BET-SA, (**c**) BJH desorption curve for pore volume and average pore size distribution

to H-C-H symmetric bending [47], H-C-H bending, H-O-H vibrations [4], OH Surface hydroxyl group of TiO_2 [48], N-H stretching of amines and amides, NH_2 stretching vibrations [11], water O-H stretching vibrations respectively.

In comparison to this adsorbent after adsorption FTIR spectra (Fig. 4 (b)) shows similar peaks with decrease in intensity. This decrease in intensity is attributed to the surface adsorption of anionic dye on the cationic adsorbent. Observable decrease in the intensity was observed for peaks at 440, 550 cm^{-1} highlighting contribution of positively charged surface species in adsorption process.

3.5 Screening of synthesized adsorbent for adsorption of 5ppm methyl orange (MO) solution

Known weight of GR carbon, GR carbon with TiO_2 (1:1), GR carbon with TiO_2 (1:2) and GR Carbon with TiO_2(1:1) and Eu^{3+} were screened for adsorption of MO. Complete adsorption of MO is achieved by all the three adsorbents except GR carbon. However, the time required for complete removal is least for GR/TiO_2(1:1)/Eu^{3+}. The graph representing percent adsorption of MO by various synthesized adsorbent is shown as Fig. 5. However, when the percent adsorption of MO is compared for time required, it is found that RG C/TiO_2/(1:1)/Eu^{3+} requires only 2 min 24 s in comparison to RG C/TiO_2/(1:1) and RG C/TiO_2/(1:2) which is 4 min 54 s and 8 min 48 s respectively. Therefore RG C/TiO_2/(1:1)/Eu^{3+} adsorbent was synthesized with varying Eu^{3+} loading.

3.6 Adsorption of dye by RG C/TiO_2/(1:1)/Eu^{3+} with varying Eu loading

Considering the quick removal of dye molecule by RG C/TiO_2/(1:1)/Eu^{3+} adsorbent. In order to optimize metal loading, series of adsorbent were prepared by varying amount of Eu^{3+} such as RG C/TiO_2(1:1)/ Eu (0.5%), RG C/TiO_2(1:1)/ Eu (0.75%), RG C/TiO_2(1:1)/ Eu (1%), RG C/TiO_2(1:1)/ Eu (1.25%) and RG C/TiO_2(1:1)/ Eu (1.5%). These synthesized adsorbents were further screened for quick and effective dye

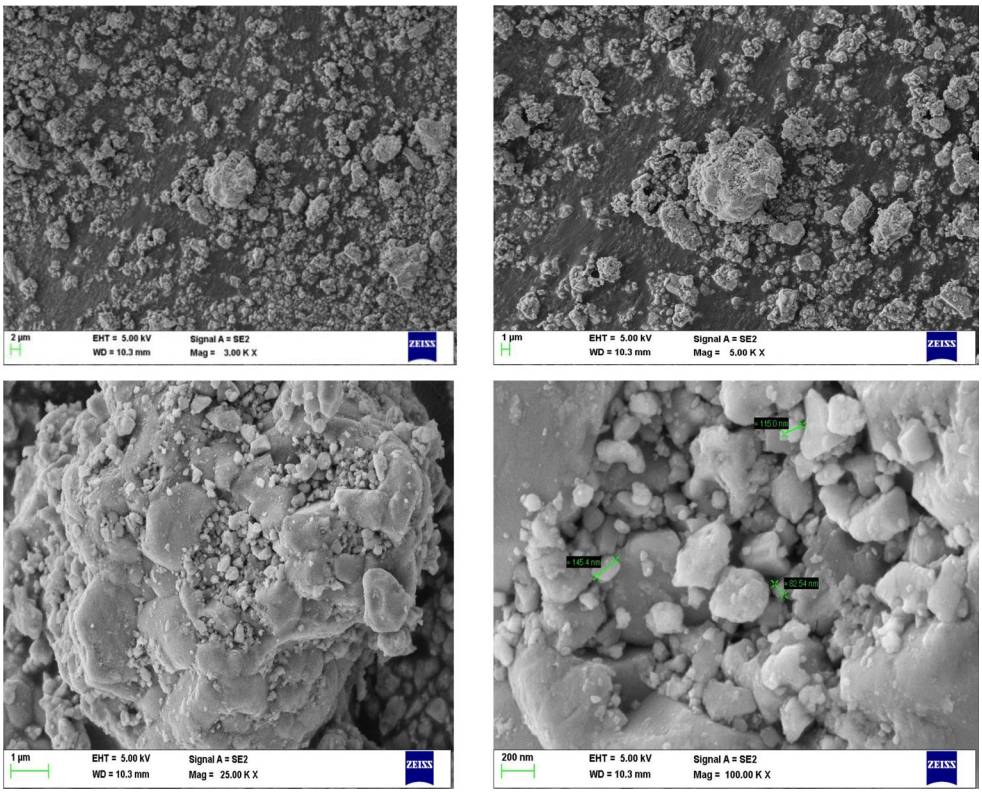

Fig. 3 Scanning Electron microscopic images of C-GR/TiO_2 (1:1)/Eu(1%)

removal by using 5ppm MO dye solution. Figure 6 shows the screening results of adsorbent with varying Eu loading.

However, the comparison cannot be completed without time required for adsorption (Series 2, Fig. 6). The time required for 93.49% adsorption of MO by RG C/TiO_2/ (1:1)/Eu^{3+} (1%) is least (134 s) than the any other adsorbent. Setting the criteria of maximum adsorption in less time RG C/TiO_2/(1:1)/Eu^{3+} (1%) found to be more effective adsorbent amongst all. Therefore, this adsorbent was further studied in detail.

3.7 Effect of adsorbent dose

RG C/TiO_2/(1:1)/Eu^{3+} (1%) was studied for optimum adsorbent dose by varying the amount of adsorbent from 25 to 125 mg for MO adsorption by keeping other parameters such as concentration of dye, volume and time of contact constant i.e. 5ppm, 10mL and 5 min respectively. Figure 7 shows % adsorption of MO at different adsorbent dose. From the figure it is observed that as the dose increases, % adsorption also increases as we go from 25 mg to 75 mg, further increase in a dose of adsorbent % of adsorption remains unchanged. Therefore, the optimum dose of adsorbent was found to be 75 mg. Increase in adsorption with increase in a dose is attributed to availability of more surface adsorption sites.

3.8 Effect of MO concentration

The dye concentration was varied from 5 to 30 ppm and its effect on the adsorption capacity of a shortlisted adsorbent was studied by keeping other parameters constant such as adsorbent dose (75 mg), volume (10mL) and contact time (5 Min). Figure 8 shows the effect of MO concentration change on adsorption capacity of adsorbent. It was observed from the graph that as the concentration of MO is increased from 5 ppm to 10 ppm no change in the adsorption capacity of adsorbent was observed but further increase in the concentration results into slight decrease in the adsorption capacity, or we can say that the capacity is almost comparable till 25 ppm and there is decrease in the capacity as the concentration is reached to 30ppm. Decrease in the adsorption with increase in dye concentration is due to limited availability of unsaturation sites present on the adsorbent however the higher adsorption capacity shown by the adsorbent can be due to mesororous highly crystalline and nano sized adsorbent also surface doping of positively charged Eu^{3+} to attract anionic dye.

3.9 Effect of pH on adsorption

Adsorption of dye at different pH i.e. from 2 to 9 was studied at optimum adsorbent dose i.e. 75 mg, MO concentration of 5ppm, volume 10mL, agitation speed 150 rpm and

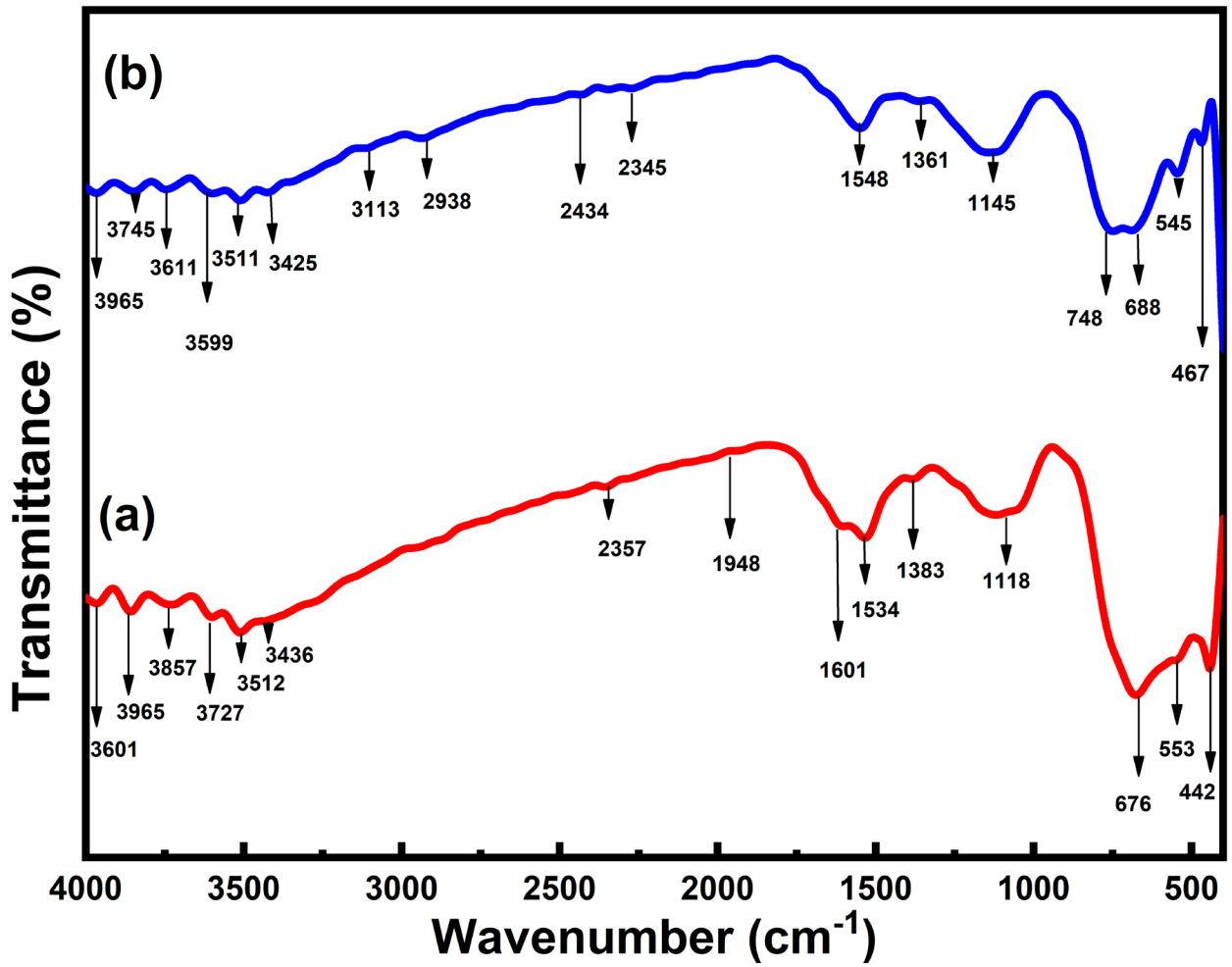

Fig. 4 FTIR spectra of C-GR/TiO_2 (1:1)/Eu(1%) (**a**) before and (**b**) after adsorption of Methyl Orange dye

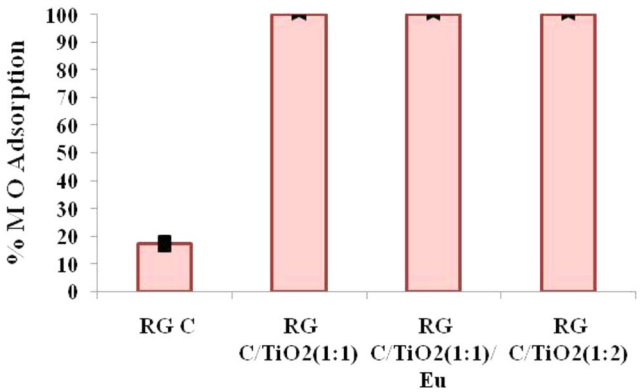

Fig. 5 Screening of synthesized absorbent for dye adsorption (Initial MO concentration = 5ppm, volume = 10mL, adsorbent dose = 75 mg. agitation speed = 150 rpm)

at 32-33°C. Figure 9 Shows effect of pH changes on dye adsorption by the synthesized adsorbent. From the figure it is clear that the dye removal is favourable from acidic to neutral in the range of 97.95–100% adsorption. Slight decrease in the removal capacity was observed as the pH shifts towards alkaline side i.e. 95.34% removal rate at pH 9. This is because adsorption is based on forces of attraction between anionic dye and cationic adsorbent; presence of acidic environment is favourable for the process. However very slight decrease in the adsorption capacity with shift in pH towards alkaline side, shows usability of adsorbent at all pH conditions for treating dye present in water or waste water.

3.10 Adsorption isotherms

Adsorption isotherm is the relationship between the equilibrium concentration of adsorbate and amount adsorbed on adsorbent at constant temperature; process designing highlights the significance of adsorption isotherms. Adsorption of MO by RG-C/TiO_2/(1:1)/Eu^{3+} (1%) adsorbent was further studied for different isotherm models in order to evaluate adsorption capacity, surface and binding properties of the synthesized adsorbent. Isothermal studies were carried

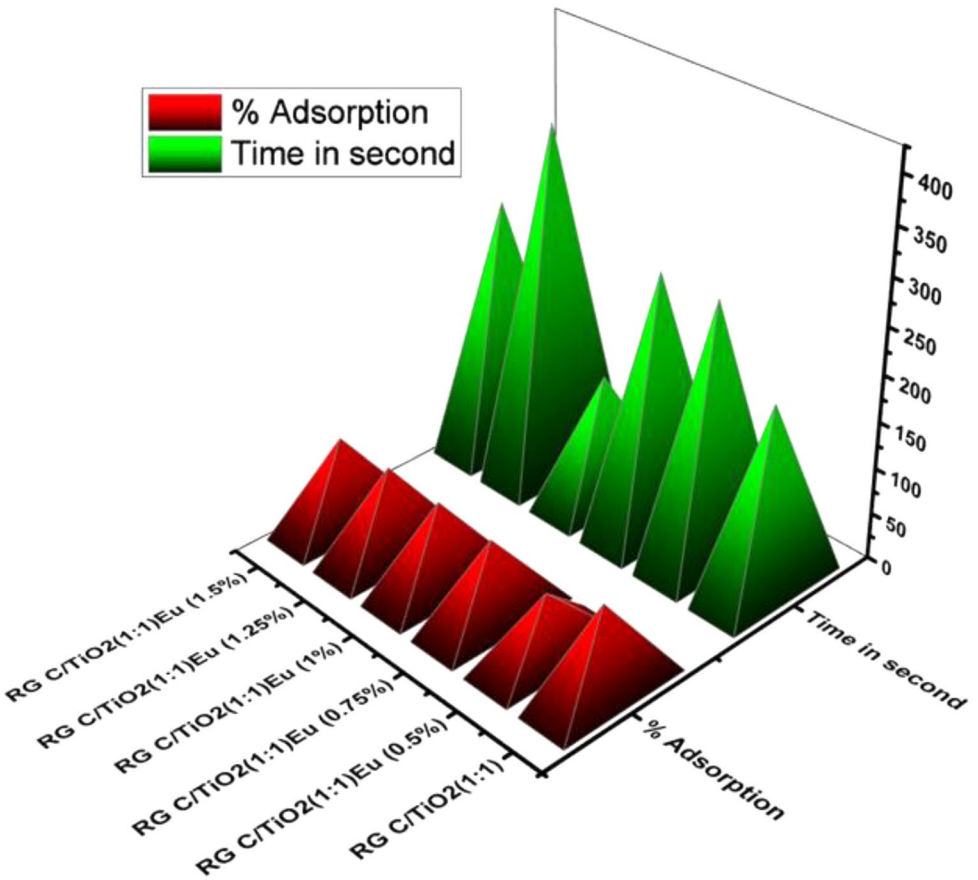

Fig. 6 Screening RG C/TiO_2/(1:1)/Eu^{3+} with varying Eu loading for dye adsorption and Time required for adsorption (Initial MO concentration = 5ppm, volume = 10mL, adsorbent dose = 75 mg. agitation speed = 150 rpm)

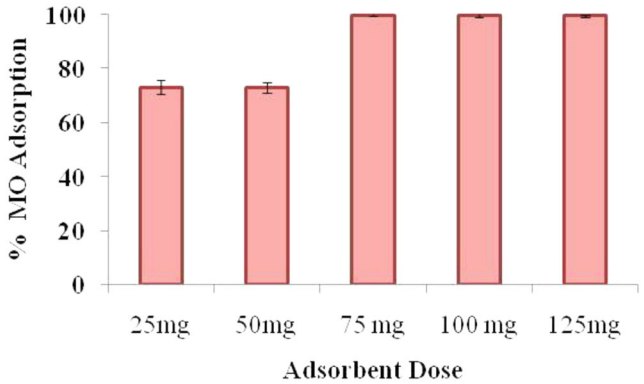

Fig. 7 Effect of adsorbent dose on MO adsorption (Initial MO concentration = 5ppm, volume = 10mL, duration = 5 min. agitation speed = 150 rpm)

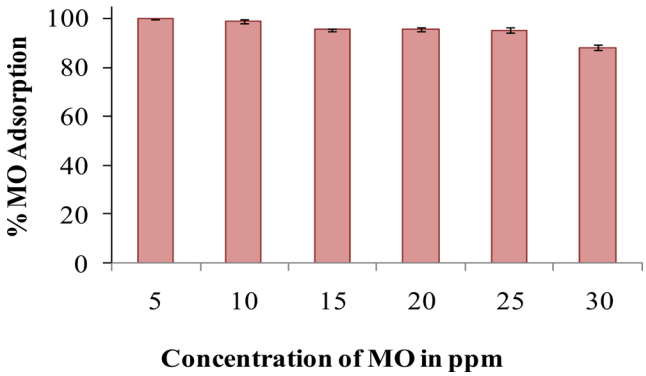

Fig. 8 Effect of MO Concentration variation on adsorption (Volume = 10mL, adsorbent dose = 75 mg, duration = 5 min. agitation speed = 150 rpm)

out for MO concentration range of 5–30 ppm at 303 K temperature with adsorbent dose of 75 mg for 10 mL of dye solution, pH = 7 and at 150 rpm agitation speed.

Langmuir and Freundlich adsorption isotherms were studied in order to determine adsorption capacity, surface binding properties and feasibility or reaction process by using synthesized adsorbent. Langmuir adsorption isotherm supports monolayer adsorption pattern on homogeneous sites however Freundlich isotherm demonstrates multilayer adsorption on heterogeneous sites [49, 50]. Temkin and D-R adsorption models were also tried for determining type of and spontaneity of adsorption. Figure 10 shows graph for (a) Langmuir, (b) Freundlich, (c) Temkin and (d) D-R adsorption isotherm. Results of isotherm parameters for all the isotherms are presented in Table 1.

Results obtained from graphs indicate that Langmuir adsorption isotherm model is more suitable for this adsorbent with R^2 value of 0.97 than fruendlich with R^2 value

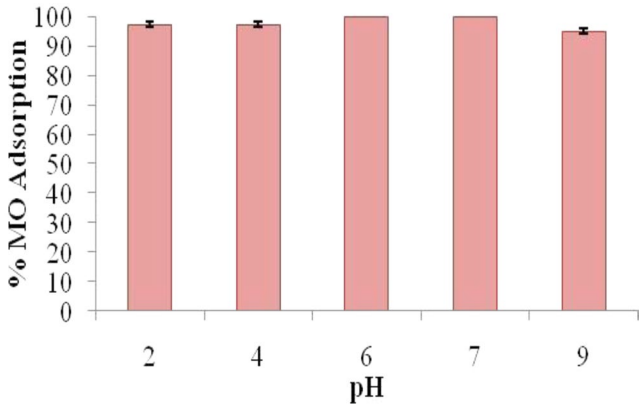

Fig. 9 Effect of pH on adsorption of Methyl Orange dye (Initial MO concentration = 5ppm, volume = 10mL, adsorbent dose = 75 mg, duration = 2.5 min. agitation speed = 150 rpm)

Table 1 Isotherm parameters:

Type of isotherm	Parameter	Values
Langmuir	q_{max} (mg/g)	2.5
	K_L (L/mg)	22.22
	R_L	0.074
	R^2	0.971
Freundlich	K_f	2.290
	1/n	0.256
	R^2	0.919
Temkin Model	B_T (J. mol^{-1})	0.39767
	K_T (L mg^{-1})	368.8919
	R^2	0.9072
Dubinin – Radushkevich (D-R)	qm (mg/g)	2.4390
	β (mol^2/K^2J^2)	1.2424E-08
	E (KJ/mol)	6343.8
	R^2	0.9400

of 0.91. Langmuir adsorption isotherm confirms the monolayer adsorption of dye onto the surface of adsorbent with q_{max} value 2.5 mg/g. R_L value is greater than zero and less than 1 indicating that the process is favorable [51, 52], also the value is very close to zero therefore the process may be irreversible [53]. High K_L value of Langmuir constant indicates greater affinity of synthesized adsorbent towards anionic dye molecule [54]. Fruendlich isotherm constant K_f indicates approximate adsorption capacity of 2.290 and value of 1/n is less than 1 corresponds to normal adsorption process.

Temkin model of adsorption is based on the assumption that as the process precedes heat of adsorption decreases linearly. The distribution of binding energy is uniform till the highest binding energy is reached. Equilibrium binding constant or maximum binding energy (K_T) value was found to be 368.8919 L mg^{-1} and Temkin isotherm constant B_T value was found to be 0.3976 J. mol^{-1} with $R^2_{=}$ 0.9072. Lower B_T value corresponds to weak interaction between adsorbet

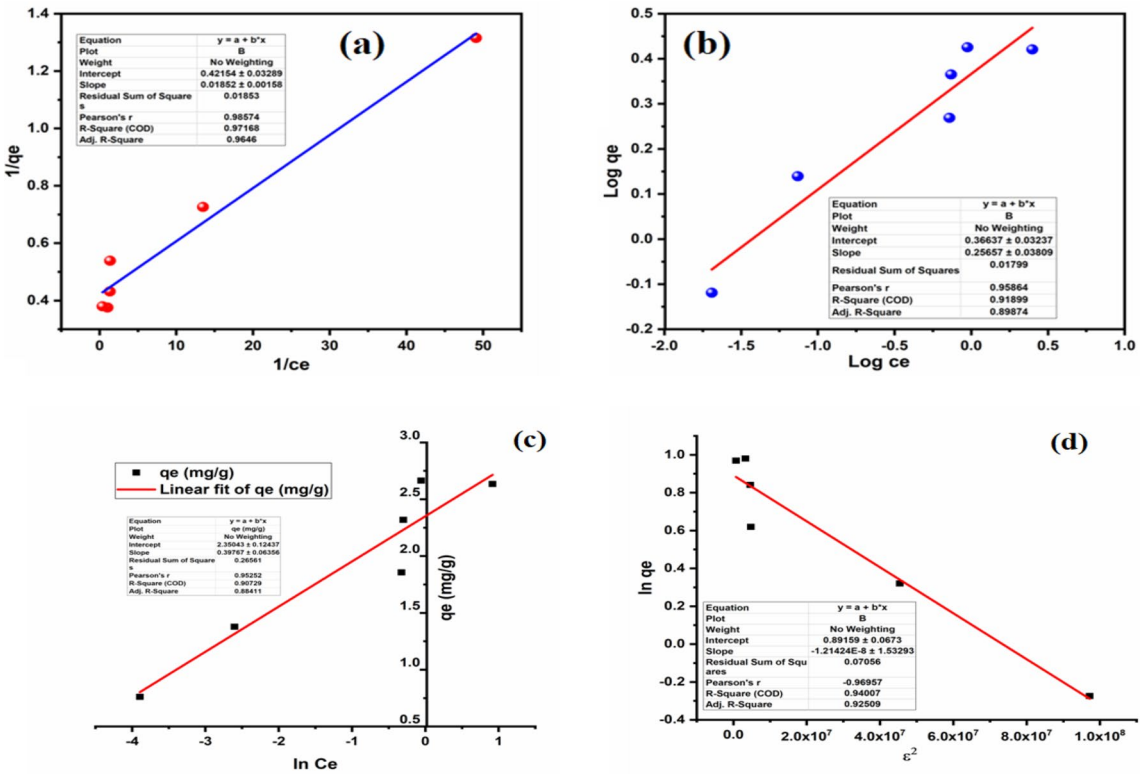

Fig. 10 (**a**) Langmuir adsorption isotherm, (**b**) Freundlich adsorption isotherm (**c**) Temkin adsorption isotherm and (**d**) D-R adsorption isotherm

and adsorbent. Dubinin–Radushkevich (D-R) isotherm was generally studied for analysing whether the process is physisorption or chemisorption. However in contrast, isotherm constant E value was found to be 6343 KJ/mol i.e. higher than 8 KJ/mol indicating the process is chemical in nature [55]. Presence of TiO_2 into the adsorbent framework can be the reason for this [27].

3.11 Thermodynamic studies

Spontaneity of the process is mostly determined by studying thermodynamic parameters such as Gibb's free energy change ΔG°, enthalpy change ΔH° and entropy change ΔS°. Experimental data obtained at different temperature is use to analyse behaviour of each thermodynamic parameter and feasibility of adsorption of MO dye by synthesized adsorbent. For this adsorption study was carried out at three different temperatures 30, 40 and 50 °C for three different MO dye concentration i.e. 5, 15 and 25 ppm. Other experimental parameters were kept constant i.e. adsorbent dose = 75 mg, pH = 7, stirring speed = 150 rpm and duration = 2.5 min.

Thermodynamic parameters for the adsorption process are calculated by using following equations;

$$\Delta G^{\circ} = -RTlnK_D \tag{2}$$

Where, R = Gas constant = 8.314 J/K Mol.

T = Absolute temperature in °K.

K_D = Equilibrium constant.

Equilibrium constant K_D is determined by following equation.

$$K_D = qe/Ce \tag{3}$$

Where q_e = amount of dye adsorbed on adsorbent.

C_e = amount of dye remaining in the solution at equilibrium.

Other thermodynamic parameters such as enthalpy and entropy are determined by following Eq. 4

$$\ln k = \frac{\Delta G^{\circ}}{RT} = \frac{\Delta H^{\circ}}{RT} + \frac{\Delta S^{\circ}}{RT} \tag{4}$$

In order to determine thermodynamic parameters experimentally, graph was plotted against 1/T and ln K_D for each concentration at different temperatures and presented in Fig. 11. Slope and intercept of graph are used to calculate enthalpy ΔH° and entropy ΔS° values. Results represented in Table 2.

Negative ΔG^{o} values indicates spontaneous adsorption process, values are in the range of -12.81 to -17.77 KJ. mol^{-1} i.e. below −20 KJ. mol^{-1}. Usually, values in the range of 0 to -20 KJ. mol^{-1} represents adsorption by weak physical interactions between adsorbate and adsorbent [56]. In this study weak forces of attraction such as electrostatic force of

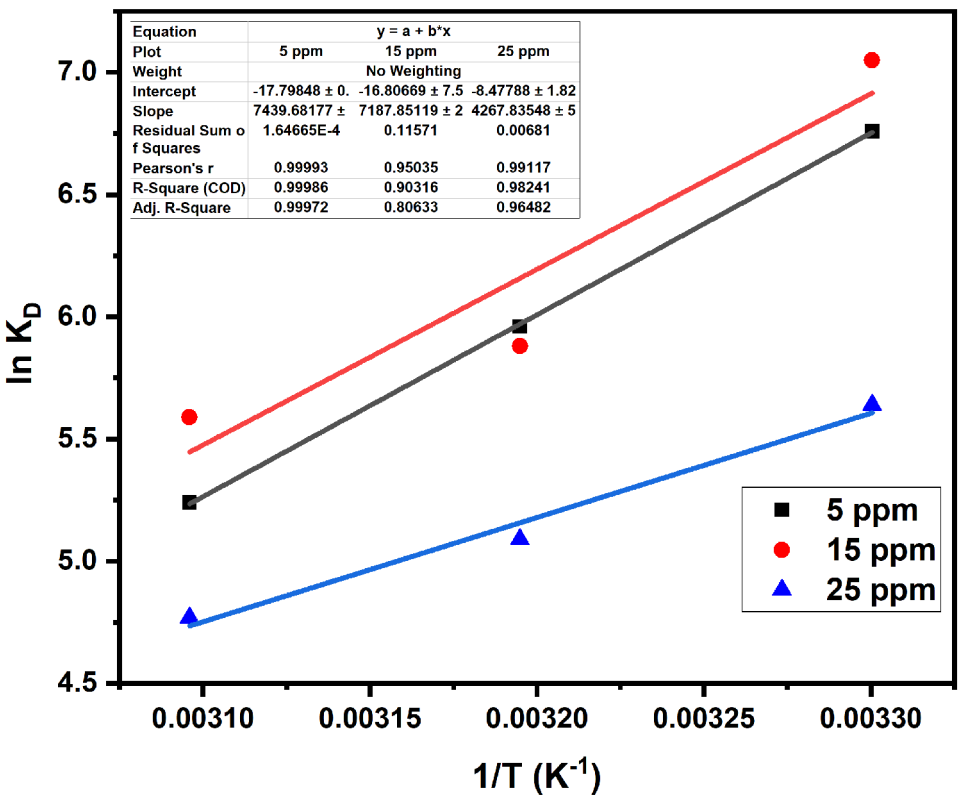

Fig. 11 Thermodynamic study for MO adsorption by using RG-C/TiO_2/(1:1)/Eu^{2+} (1%) adsorbent

Table 2 Thermodynamic parameters of Methyl orange dye adsorption process by using RG-C/TiO_2/(1:1)/Eu^{3+} (1%) adsorbent

MO Concentration (ppm or mg/L)	ΔH° (KJ. mol^{-1})	ΔS° (J. mol^{-1})	ΔG° (KJ. mol^{-1})		
			303 K	313 K	323 K
5	-61.85	-147.98	-17.0325	-15.5353	-14.0772
15	-59.76	-139.73	-17.7723	-15.3052	-15.0325
25	-35.48	-70.49	-14.2136	-13.2542	-12.8127

attraction, Hydrogen bonding may be considered as physical forces of interactions responsible for adsorption process as evidenced by FTIR spectra. Decrease in ΔG° values was observed with respect to increase in temperature. This decrease in values of ΔG° at higher temperature indicates less feasibility of adsorption with rise in temperature. Values calculated from graph for ΔH° are negative indicating that the adsorption process is exothermic in nature [57]. Calculated Entropy values are also negative representing reduction in the random collision of adsorbent and dye molecule interactions during surface adsorption process [7].

3.12 Kinetic study

Adsorption kinetics was studied for RG-C/TiO_2/(1:1)/Eu^{3+} (1%) adsorbent at optimized conditions, time requied for complete adsorption is very less here hence kinetics can be only studied up to 3 min with every 15 s time interval. Figure 12 shows (a) Pseudo first order and (b) pseudo second order kinetic diagrams for MO adsorption. Kinetic contants and parameters are presented in Table 3.

Pseudo first order kinetic results shows lower $q_{e\ (Cal)}$ value than experimentally calculated $q_{e\ (exp)}$ therefore reaction kinetics can not be well explained by pseudo first order reaction. $q_{e\ (Cal)\ by}$ pseudo second order is good agreement with the $q_{e\ (exp)}$. The correlation coefficient of pseudo second order reaction value is 0.9955 which is higher than pseudo second order reaction kinetics ($R^2 = 0.9167$). So the kinetic study confirms more inclination of adsorption kinetics towards pseudo second order model [58].

Table 3 Kinetic constant and parameters for adsorption of MO dye by RG-C/TiO_2/(1:1)/Eu^{3+} (1%) adsorbent :

Model	Parameter	Values
Pseudo first order	$q_{e\ (Cal)}$ ($mg.g^{-1}$)	0.2287
	K_1	-0.2357
	R^2	0.9167
Pseudo second order	$q_{e\ (Cal)}$ ($mg.g^{-1}$)	0.7616
	K_2	8.097
	R^2	0.9955

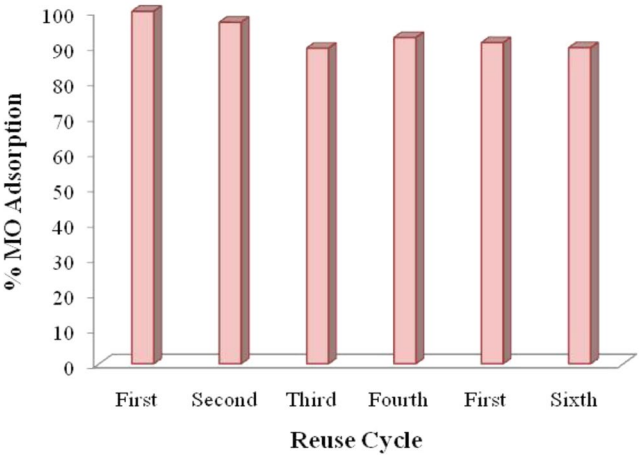

Fig. 13 Reuse and stabilization study (Initial MO concentration = 5ppm, volume = 10mL, adsorbent dose = 75 mg, duration = 2.5 min. agitation speed = 150 rpm)

3.13 Stability and reuse study

Synthesized adsorbent was also studied for reuse at room temperature (32-33°C), with following experimental conditions MO concentration = 5ppm, volume = 10mL, pH = 7, adsorbent dose = 75 mg contact time = 2.5 min agitation speed = 150 rpm. Figure 13 shows adsorption of dye up to six reuse cycle under above said conditions. From the graph it can be easily understood that the catalyst can be reused and the % adsorption is almost maintained up to six consecutive cycles. Adsorption remains same during first and second reuse i.e. 100 to 96.89%. The adsorption decreases slightly

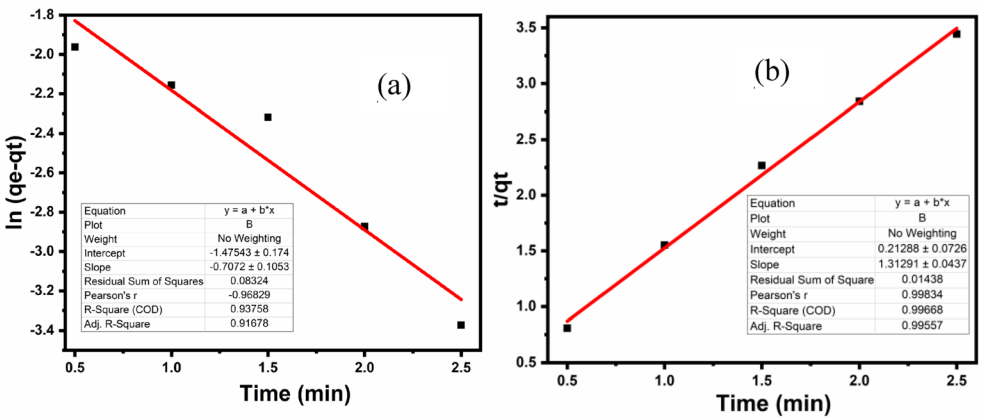

Fig. 12 (**a**) Pseudo first order and (**b**) pseudo second order kinetic diagrams for MO adsorption

but remains almost constant i.e. between 92.5 and 89.5% from third to sixth reuse cycle. SEM data reveals small size and irregular morphology of adsorbent grains, indicating presence of more defects on the surface this might be facilitating extra ordinarily high reuse capacity of the synthesized bioadsorbent. Mesoporousity and presence of more positive species/ions on the surface of adsorbent could be another reason for consistency in reuse result. From this we can conclude that, the synthesized adsorbent was found quite stable up to six consecutive reuse cycles and can be reused easily without decrease in the adsorption efficiency.

4 Possible mechanism of adsorption

Chemical name of Methyl orange is p(((p-dimethylamino) phenyl)azo)benzenesulphonic acid sodium salt. It is water soluble dye when it is dissolved in water it get dissociated as,

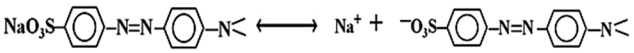

Dye molecule remains anionic dye ions in aqueous solution. Synthesized adsorbent is doped with Eu^{3+} with formation Ti-O-Eu^{3+} species on the surface [59] so the adsorbent molecule is + vely charged. High columbic force of attraction between the anionic dye molecule and cationic adsorbent may be the probable reason for high efficiency of adsorption [47, 60]. Columbic attraction can also be observed between the positively charged O-Ti and NH^+, NH_2^+ groups. Hydrogen bonding between surface water molecules, OH groups with Nitrogen present in the azo group of a dye also facilitates adsorption. n-π interaction can also possible between lone pair present on oxygen atom and pi electrons of benzene ring present in MO frame work [47]. Chemisorption characteristic of titanium surface is responsible for formation of Ti-OH and dissociative Ti-OH_2^+ in the presence of water via interfacial electron transfer [27]. Presence of such positive species may also contribute into adsorption process.

Exceptionally high adsorption capacity is attributed to surface defects, mesoporous material with surface functional groups and titania frame work. Figure 14 depicts possible adsorption mechanism of MO dye by synthesized RG-C/TiO2/(1:1)/Eu3+ (1%) adsorbent.

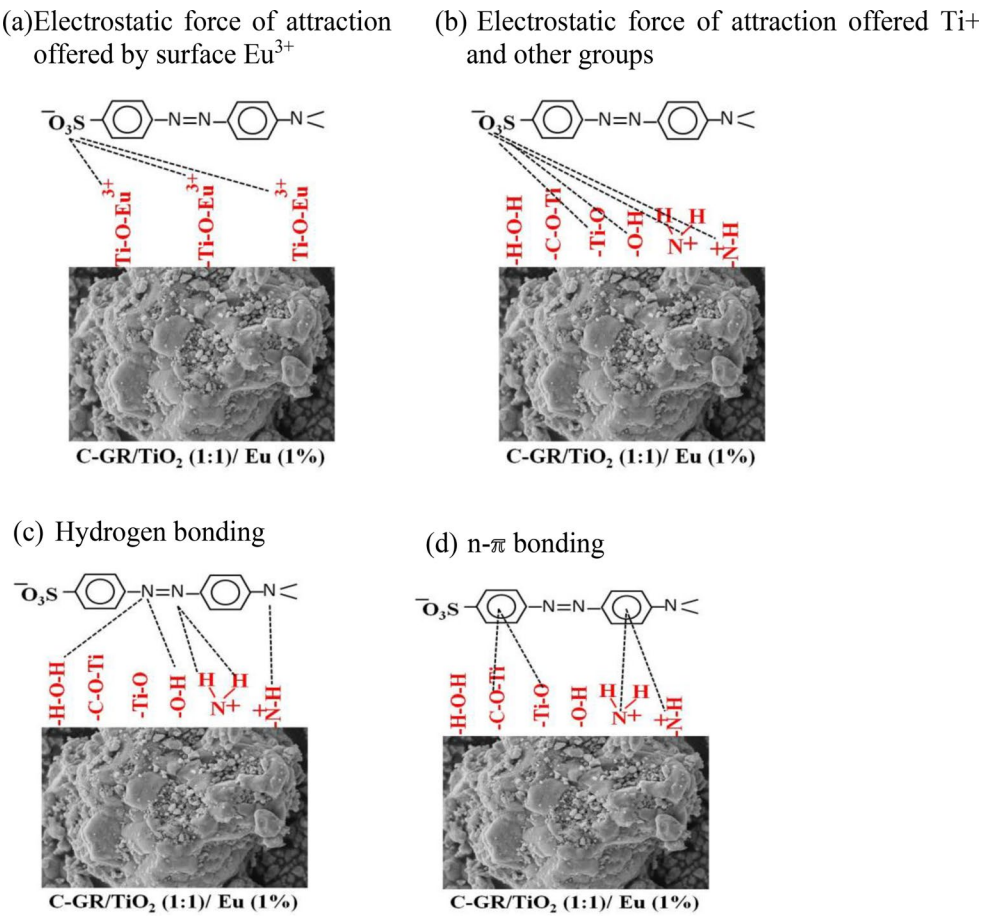

Fig. 14 Possible adsorption mechanism of MO dye by synthesized RG-C/TiO_2/(1:1)/Eu^{2+} (1%) adsorbent

5 Conclusion

Environmental benign and dairy waste *ghee* residue was used as a support and source of carbon on to which TiO_2 was supported and Eu was doped. Permutations and combinations were also carried out while synthesizing the adsorbent with respect to Gr/TiO_2 ratio and doping percentage. The synthesized composites were characterized for X-ray diffraction, Surface area, pore size and pore volume, surface morphology and FTIR. The XRD data confirms formation of crystalline anatase phase of titania with nanosized particles. SEM image also supports formation of particles in nanometer range with irregular morphology. BET-surface area of GR-c/TiO_2/Eu^{3+} (1%) was found to be 53.633 m²/g with total pore volume = 8.555e-02 cc/g for pores smaller than 18330.1 Å (Radius) at P/Po = 0.99948 and average pore radius was found to be 3.19022e + 01 Å, indicating formation of mesoporous adsorbent. FTIR shows presence of Eu-O, TiO_2, Ti-O, Ti-O-C bonds and N-H and NH_2 bonds. The as synthesized adsorbents were screened for adsorption of methyl orange dye with concentration of 5ppm. Quick and complete removal was observed for RG C/TiO_2/(1:1)/Eu^{3+} (1%) adsorbent in less than 3 min. i.e. in 2 min 24 s. Shortlisted adsorbent was then subjected to optimization of operational parameters such as dose of adsorbent and concentration of dye. Best results were obtained with very low catalyst dosage of 75 mg/10mL with dye concentration of 5ppm. Adsorbent was also studied with respect to different adsorption isotherm; isotherm data reveals that Langmuir adsorption isotherm model is more suitable with R^2 value of 0.97. This indicates monolayer adsorption of dye molecule on synthesized biogenic adsorbent. Thermodynamic studies were also carried out negative ΔG^o, ΔH^o values assures spontaneity and feasibility of process. Pseudo first and second order reaction kinetics models were also studied for analysing kinetic behaviour of adsorption process. The kinetic model of pseudo second order having higher R^2 value and $q_{e\ (Cal)\ value}$ is in good agreement with $q_{e\ (exp)}$. Reuse and stability study was also carried out and the biogenic adsorbent was found quite stable up to six reuse cycles with effective adsorption efficiency.

Acknowledgements One of the authors MVJ is grateful to the Principle of Shri Ramdeobaba College of Engineering and Management, Nagpur for constant support and encouragement.

Author contributions Meenal Joshi: Conceptualization, methodology, investigation, validation, writing-original manuscript. Abhijeet Kadam: Conceptualization, methodology, writing-review and editing manuscript. S.J. Dhoble: Supervision, writing.

Funding Not applicable.

Data availability No datasets were generated or analysed during the current study.

Declarations

Ethical approval Not applicable.

Competing interests The authors declare no competing interests.

References

1. Maheshwari, K., Agrawal, M., Gupta, A.B.: Dye pollution in water and waste water, in Novel Materials for Dye-containing Wastewater Treatment Springer, Page No. 1–25, (2021). https://doi.org/10.1007/978-981-16-2892-4_1
2. Khattab, T.A., Abdelrahman, M.S., Rehan, M.: Textile dyeing industry: Environmental impacts and remediation. Environ. Sci. Pollut Res. **27**, 3803–3818 (2020). https://doi.org/10.1007/s11356-019-07137-z
3. Aquino, J.M., Rocha-Filho, R.C., Ruotolo, L.A., Bocchi, N., Biaggio, S.R.: Electrochemical degradation of a real textile wastewater using β-PbO2 and DSA®. Anodes Chem. Eng. J. **251**, 138–145 (2014). https://doi.org/10.1016/j.cej.2014.04.032
4. Foroutan, R., Peighambardoust, S.J., Boffito, D.C., Ramavandi, B.: Sono-Photocatalytic activity of Cloisite 30B/ZnO/Ag2O nanocomposite for the Simultaneous Degradation of Crystal Violet and Methylene Blue Dyes in Aqueous Media. Nanomaterials. **12**, 3103 (2022). https://doi.org/10.3390/nano12183103
5. Haque, M.M., Haque, M.A., Mosharaf, M.K., Marcusa, P.K.: Decolorization, degradation and detoxification of carcinogenic sulfonated azo dye methyl orange by newly developed biofilm consortia. Saudi J. Biol. Sci. **28**(1), 793–804 (2021). https://doi.org/10.1016/j.sjbs.2020.11.012
6. Bafana, A., Chakrabarti, T., Saravana Devi, S.: Azoreductase and dye detoxification activities of Bacillus velezensis strain AB. Appl. Microbiol. Biotechnol. **77**, 1139–1144 (2008). https://doi.org/10.1007/s00253-007-1212-5
7. Dutta, S.K., Amin, M.K., Ahmed, J., Elias, M., Mahiuddin, M.: Removal of toxic methyl orange by a cost-free and eco-friendly adsorbent: Mechanism, phytotoxicity, thermodynamics, and kinetics. South. Afr. J. Chem. Eng. 40. 195–208 (2022). https://doi.org/10.1016/j.sajce.2022.03.006
8. Shah, S.S., Sharma, T., Dar, B.A., Bamezai, R.K.: Adsorptive removal of methyl orange dye from aqueous solution using populous leaves: Insights from kinetics, thermodynamics and computational studies. Environ. Chem. Ecotoxicol. **3** (2021). 172–18 https://doi.org/10.1016/j.enceco.2021.05.002
9. Raji, F., Zafari, M., Rahbar-Kelishami, A.: Enhanced removal of methyl orange using modified anion exchange membrane adsorbent. Int. J. Environ. Sci. Technol. **20**, 9823–9836 (2023). https://doi.org/10.1007/s13762-023-05089-z
10. Oturan, M.A., Aaron, J.J.: Advanced Oxidation Processes in Water/Wastewater treatment: Principles and applications. A review. Crit. Rev. Environ. Sci. Technol. **44**(23), 2577–2641 (2014). https://doi.org/10.1080/10643389.2013.829765
11. Joshi, M.M., Labhsetwar, N.K., Mangrulkar, P.A., Tijare, S.N., Kamble, S.P., Rayalu, S.S.: Visible light induced photoreduction of methyl orange by N-doped mesoporous titania. Appl. Catal. A. **357**, 26–33 (2009). https://doi.org/10.1016/j.apcata.2008.12.030
12. Vucurovic, V.M., Razmovski, R.N., Miljic, U.D., Puskas, V.S.: Removal of cationic and anionic dyes from aqueous solutions by adsorption on maize stem tissue. J. Taiwn Inst. Chem. Eng. **45**(4), 1700–1708 (2014). https://doi.org/10.1016/j.jtice.2013.12.020
13. Aguayo-Villarreal, I.A., Ramírez-Montoya, L.A., Hernández-Montoya, V., Bonilla-Petriciolet, A., Montes-Moránc, M.A., Ramírez-López, E.M.: Sorption mechanism of anionic dyes

on pecan nut shells (Carya illinoinensis) using batch and continuous systems. Ind. Crops Prod. **48**, 89–97 (2013). https://doi.org/10.1016/j.indcrop.2013.04.009
14. Xie, B., Qin, J., Wang, S., Li., X., Sun, H., Chen, W.: Adsorption of Phenol on Commercial activated carbons: Modelling and Interpretation. Int. J. Environ. Res. Public. Health. **17**(3), 789 (2020). https://doi.org/10.3390/ijerph17030789
15. Önal, Y.: Kinetics of adsorption of dyes from aqueous solution using activated carbon prepared from waste apricot. J. Hazard. Mater. **137**, 1719–1728 (2006). https://doi.org/10.1016/j.jhazmat.2006.05.036
16. Tahir, N., Bhatti, H.N., Iqbal, M., Noreen, S.: Biopolymers composites with peanut hull waste biomass and application for Crystal Violet adsorption. Int. J. Biol. Macromol. 94(Pt A). 210–220 (2017). https://doi.org/10.1016/j.ijbiomac.2016.10.013
17. Rahaman, M.H., Islam, M.A., Islam, M.M., Md. Rahman, A., Nur Alam, S.M.: Biodegradable composite adsorbent of modified cellulose and chitosan to remove heavy metal ions from aqueous solution. Curr. Res. Green. Sustainable Chem. **4**, 100119 (2021). https://doi.org/10.1016/j.crgsc.2021.100119
18. Aichour, A., Zaghouane-Boudiaf, H., Mohamed Zuki, F.B., Aroua, M.K., Ibbora, C.V.: Low-cost, biodegradable and highly effective adsorbents for batch and column fixed bed adsorption processes of methylene blue. J. Environ. Chem. Eng. **7**(5), 103409–103413 (2019). https://doi.org/10.1016/j.jece.2019.103409
19. Malik, R., Ramteke, R.D., Wate, S.R.: Adsorption of malachite green on groundnut shell waste based powdered activated carbon. Waste Manage. **27**(9), 1129–1138 (2007). https://doi.org/10.1016/j.wasman.2006.06.009
20. Khammour, F., Abdoul-Latif, F.M., Ainane, A., Mohamed, J., Ainane, T.: Eco-friendly adsorbent from Waste of Mint: Application for the removal of Hexavalent Chromium. J. Chem. (2021). https://doi.org/10.1155/2021/8848964
21. Kirti, S., Bhandari, V.M., Jena, J., Sorokhaibam, L.G., Bhattacharyya, A.S.: Exploiting functionalities of biomass in nanocomposite development: Application in dye removal and disinfection along with process intensification. Clean Technol. Environ. Policy. **20**(5), 981–994 (2018). https://doi.org/10.1007/s10098-018-1519-1
22. Sousa, R.M., de Araújoa, R., da Silva Ferreira, T.H., Napoleão, L.C.B., Barroso Coelho, M.T., dos Santos Correia, M.L., Vilela Oliva, P.M.: Guedes Paivaa, Crataeva tapia bark lectin is an affinity adsorbent and insecticidal agent, Plant Science, 183 20–26. (2012). https://doi.org/10.1016/j.plantsci.2011.10.018
23. Rekha Krishnan, G., Prabhakaran, K., George, B.K.: Biogenic magnetic nano hydroxyapatite: Sustainable adsorbent for the removal of perchlorate from water at near-neutral pH. J. Environ. Chem. Eng. **9**(6), 106316 (2021). https://doi.org/10.1016/j.jece.2021.106316
24. Batool, A., Valiyaveettil, S.: Chemical transformation of soya waste into stable adsorbent for enhanced removal of methylene blue and neutral red from water. J. Environ. Chem. Eng. **9**, 104902 (2021). https://doi.org/10.1016/j.jece.2020.104902
25. Valente, N.J.M., Laginhas, C.E.C., Carrott, P.J.M., Ribeiro, M.M.L., Carrott: Production of activated carbons from almond shell, Fuel Processing Technology, 92 (2) 234–240. (2011). https://doi.org/10.1016/j.fuproc.2010.03.024
26. Han, Z., Kong, S., Cheng, J., Sui, H., Li, X., Zhang, Z., He, L.: Preparation of efficient Carbon-based Adsorption Material using asphaltenes from Asphalt Rocks. Ind. Eng. Chem. Res. **58**, 14785–14794 (2019). https://doi.org/10.1021/acs.iecr.9b02143
27. Shila Jafari, M., Sillanpää: Adsorption of dyes on modified TiO_2 Advanced Water Treatment. https://doi.org/10.1016/B978-0-12-819216-0.00002-3
28. Asuha, S., Zhou, X.G.: Zhao Adsorption of methyl orange and cr(VI) on mesoporous TiO_2 prepared by hydrothermal method. J. Hazard. Mater. **15**(181), 204–210 (2010). https://doi.org/10.1016/j.jhazmat.2010.04.117
29. Jing, C., Meng, X., Calvache, E., Jiang, G.: Remediation of organic and inorganic arsenic contaminated groundwater using a nanocrystalline TiO_2-based adsorbent. Environ. Pollut. **157**, 8–9 (2009). https://doi.org/10.1016/j.envpol.2009.03.011
30. Fialova, K., Motlochova, M., Cermakova, L., Novotna, K., Bacova, J., Rousar, T., Subrt, J., Pivokonsky, M.: Removal of manganese by adsorption onto newly synthesized TiO_2-based adsorbent during drinking water treatment. Environ. Technol. **44**(9), 1322–1333 (2023). https://doi.org/10.1080/09593330.2021.2000042
31. Orojlou, B., Zargar, S., Rastegarzadeh: Metal oxide/TiO_2 nanocomposites as efficient adsorbents for relatively high temperature H_2S removal. J. Nat. Gas Sci. Eng. **59**, 363–373 (2018). https://doi.org/10.1016/j.jngse.2018.09.016
32. Aziz, A.A., Ibrahim, S.: Preparation of Activated Carbon/N-doped Titania Composite for Synergistic Adsorption-photocatalytic Oxidation of Batik Dye, IOP Conf. Series: Materials Science and Engineering, 358, 012014. (2018). https://doi.org/10.1088/1757-899X/358/1/012014. IOP Conf. Ser.: Mater. Sci. Eng. 358 012014
33. Zhao, Y., Li, X., Tian, C., Wang, J.: Production of carbon-doped titanium dioxide (C–TiO2) from polytitanium-coagulated sludge as an adsorbent or photocatalyst for pollutant removals. J. Clean. Prod. **267**, 121979 (2020). https://doi.org/10.1016/j.jclepro.2020.121979
34. Wani, A.D., Prasad, W., Khamrui, K., Jamb, S.: A review on quality attributes and utilization of ghee residue, an under-utilized dairy by-product. Future Foods. **5**, 100131022 (2022). https://doi.org/10.1016/j.fufo.2022.100131
35. Arumugam, M.P., Vedhanayagam, K., Doraisamy, K.A., Narahari, D.: Chemical Composition and Nutritive Value of *Ghee* Residue for Chickens. Anim. Feed Sci. Technol. **26**, 119–128 (1989). https://doi.org/10.1016/0377-8401-2889-2990011-4
36. Hao, L., Desai, M.K., Wang, P., Valiyaveettil, S.: Successive extraction of as(V), Cu(II), and P(V) ions from Water using Surface modified Ghee Residue protein. ACS Sustainable Chem. Eng. **5**, 3742–3750 (2017). https://doi.org/10.1021/acssuschemeng.6b02152
37. Lavasani, S.H., Sarvi, M.N.: Ebrahim Azimi Synthesis of Mesoporous Nanoparticles of TiO2 in Anatase form from Ilmenite Concentrate, 7th International conference on Materials Engineering and Metallurgy iMAT Tehran, Iran October 9–10, 2018 (2018)
38. Lusvardi, V.S., Barteau, M.A., Farneth, W.E.: The effects of Bulk Titania Crystal structure on the adsorption and reaction of Aliphatic alcohols. J. Catal. **153**(1), 41–53 (1995). https://doi.org/10.1006/JCAT.1995.1106
39. Barbour, M.E., O'Sullivan, D.J., Jagger, D.C.: Chlorhexidine adsorption to anatase and rutile titanium dioxide. Colloids Surf. A: Physicochem Eng. Aspects. **307**, 116–120 (2007). https://doi.org/10.1016/j.colsurfa.2007.05.010
40. Thamaphat, K., Limsuwan, P., Ngotawornchai, B.: Kasetsart Phase characterization of TiO_2 powder by XRD and TEM. (Nat Sci). **42**, 357–361 (2008). https://li01.tci-thaijo.org/index.php/anres/article/view/244620
41. Yadav, P., Putro, D., Kim, J., Rai, A.K.: Pom-Pom Flower-like morphology of δ-MnO2with Superior Electrochemical Performances for Rechargeable Aqueous Zinc Ion Batteries. Batteries. **9**(2), 133 (2023). https://doi.org/10.3390/batteries9020133
42. Dunicz B.L.: Surface area of activated Charcoal by Langmuir Adsorption Isotherm. J. Chem. Educ. **38**(7), 357 (1961). https://doi.org/10.1021/ed038p357
43. Xie, G., Zhang, Z., Zhang, J.: Synthesis and characterization of the novel color-tunable Eu/Tb(BPA)3phen composites. MATEC

Web Conferences. **207**, 03021 (2018). https://doi.org/10.1051/matecconf/201820703021
44. Rajakumar, G., Abdul Rahumana, A., Mohana Roopan, S., Gopiesh Khanna, V., Elango, G., Kamaraj, C., Abduz Zahir, A., Velayuthama, K.: Fungus-mediated biosynthesis and characterization of TiO_2 nanoparticles and their activity against pathogenic bacteria. Spectrochim. Acta Part A Mol. Biomol. Spectrosc. **91**, 23–29 (2012). https://doi.org/10.1016/j.saa.2012.01.011
45. Joshi, M.M., Labhsetwar, N.K., Parwate, D.V., Rayalu, S.S.: Efficient photocatalytic hydrogen generation by silica supported and platinum promoted titanium dioxide. Mater. Res. Bull. **48**, 3545–3552 (2013). https://doi.org/10.1016/j.materresbull.2013.05.057
46. Alice, Z., Stefano, C., Sara Maria, C., Paolo, C., Alberto, A., Giorgia, F.: Sucrose-based sol-gel synthesis of microporous titanium carbide as target material for the production of radioisotopes. Microporous Mesoporous Mater. **337**, 111917 (2022). https://doi.org/10.1016/j.micromeso.2022.111917
47. Sonvanshi, V., Gandhi, K., Ramani, A., Sharma, R., Seth, R.: ATR-FTIR coupled with chemometric techniques to detect vanaspati ghee (hydrogenated vegetable oil) adulteration in milk fat. Results Chem. **7**, 101343 (2024). https://doi.org/10.1016/j.rechem.2024.101343
48. Krishnan, J., Nerissa, E., Hadi, A.: Synthesis, characterization and efficiency of N, C-TiO_2 as an active visible light photocatalyst. Appl. Mech. Mater. **661**, 63–67 (2014). https://doi.org/10.4028/www.scientific.net/AMM.661.63
49. Karim-Talaq Mohammad, A., Saud Abdulhameed, A., Jawad, A.H.: Box-Behnken design to optimize the synthesis of new cross-linked chitosan-glyoxal/TiO2 nanocomposite: Methyl orange adsorption and mechanism studies. Int. J. Biol. Macromol. **129**, 98–109 (2019). https://doi.org/10.1016/j.ijbiomac.2019.02.025
50. Ayub, A., Raza, Z.A., Majeed, M.I., Tariq, M.R., Irfan, A.: Development of sustainable magnetic chitosan biosorbent beads for kinetic remediation of arsenic contaminated water International. J. Biol. Macromol. **163**(15), 603–617 (2020). https://doi.org/10.1016/j.ijbiomac.2020.06.287
51. Benali, B.M.O., Benyahia, M., Benmoussa, Y., Zenasni, M.A.: Adsorptive removal of anionic dye from aqueous solutions by Algerian kaolin: Characteristics, isotherm, kinetic and thermodynamic studies. J. Mater. Environ. Sci. **4**(3), 482–491 (2013). ISSN: 2028–2508
52. Ferreira, B.C.S., Teodoro, F.S., Mageste, A.B., Gil, L.F., Freitas, R.P., Gurgel, L.V.A.: Application of a new carboxylate-functionalized sugarcane bagasse for adsorptive removal of crystal violet from aqueous solution: Kinetic, equilibrium and thermodynamic studies. Ind. Crops Prod. **65**, 521–534 (2015). https://doi.org/10.1016/j.indcrop.2014.10.020
53. Yöntena, V., Sanyürek, N.K., Kivan, M.R.: A thermodynamic and kinetic approach to adsorption of methyl orange from aqueous solution using a low cost activated carbon prepared from Vitis vinifera L. Surf. Interfaces. **20**, 100529 (2020). https://doi.org/10.1016/j.surfin.2020.100529
54. Foroutan, R., Jamaleddin Peighambardoust, S., Ghojavand, S., Farjadfard, S., Ramavandi, B.: Cadmium elimination from wastewater using potato peel biochar modified by ZIF-8 and magnetic nanoparticle, Colloid and Interface Science Communications. 2215 – 0382. **55**, 100723 (2023). https://doi.org/10.1016/j.colcom.2023.100723
55. Demir, H., Top, A., Balkose, D., Ulku, S.: Dye adsorption behavior of Luffa cylindrica fibers. J. Hazard. Mater. **153**, 389–394 (2008). https://doi.org/10.1016/j.jhazmat.2007.08.070
56. Dada, A.O., Olalekan, A.P., Olatunya, A., Dada, O.O.: Langmuir, Freundlich, Temkin and Dubinin–Radushkevich Isotherms studies of Equilibrium Sorption of Zn 2 + unto Phosphoric Acid Modified Rice Husk. J. Appl. Chem. **3**(1), 38–45 (2012). https://doi.org/10.9790/5736-0313845
57. Jiang, R., Fu, Y.-Q., Zhu, H.-Y., Yao, J., Xiao, L.: Removal of methyl orange from aqueous solutions by magnetic maghemite/chitosan nanocomposite films: Adsorption kinetics and equilibrium. J. Appl. Polym. Sci. S2125 (2012). https://doi.org/10.1002/app.37003
58. Foroutan, R., Zareipour, R., Mohammadi, R.: Fast adsorption of chromium (VI) ions from synthetic sewage using bentonite and bentonite/bio-coal composite: A comparative study. Mater. Res. Express. **6**, 025508 (2019). https://doi.org/10.1088/2053-1591/aaebb9
59. Zenga, Q.G., Dinga, Z.J., Zhang, Z.M.: Synthesis, structure and optical properties of Eu3+/TiO2 nanocrystals at room temperature. J. Lumin. **118**, 301–307 (2006). https://doi.org/10.1016/j.jlumin.2005.09.002
60. Turan, B., Bugdayci, M., Benzesik, K., Demircivi, P.: Synthesis of Eu doped SrAl2O4 composite: Adsorption characteristics on tetracycline and ciprofloxacin antibiotics. Sep. Sci. Technol. (2021). https://doi.org/10.1080/01496395.2021.1878372